Rapid Communications

Mechanisms of screening or enhancing the pseudogap throughout the two-band Bardeen-Cooper-Schrieffer to Bose-Einstein condensate crossover

Hiroyuki Tajima,[1,2] Yuriy Yerin,[3,4] Pierbiagio Pieri,[5,6] and Andrea Perali[7]

[1]*Department of Mathematics and Physics, Kochi University, Kochi 780-8520, Japan*
[2]*RIKEN Nishina Center, Wako, Saitama 351-0198, Japan*
[3]*Dipartimento di Fisica e Geologia, Università di Perugia, I-06123 Perugia, Italy*
[4]*School of Science and Technology, Physics Division, Università di Camerino, I-62032 Camerino (MC), Italy*
[5]*Dipartimento di Fisica e Astronomia, Università di Bologna, I-40127 Bologna, Italy*
[6]*INFN, Sezione di Bologna, I-40127 Bologna, Italy*
[7]*School of Pharmacy, Physics Unit, Università di Camerino, I-62032 Camerino (MC), Italy*

(Received 9 September 2020; revised 3 November 2020; accepted 19 November 2020; published 17 December 2020)

We demonstrate the rise and fall of multiple pseudogaps in the Bardeen-Cooper-Schrieffer to Bose-Einstein condensation crossover in two-band fermionic systems having different pairing strengths in the deep band and in the shallow band. The striking features of this phenomenon are an unusual many-body screening of the pseudogap state and the importance of pair-exchange couplings, which induces multiple pseudogap formation in the two bands. The multiband configuration suppresses pairing fluctuations and the pseudogap opening in the strongly interacting shallow band at small pair-exchange couplings by screening effects, with a possible connection to the pseudogap phenomenology in iron-based superconductors. On the other hand, the multiple pseudogap mechanism is accompanied by the emergence of binary preformed Cooper pairs originating from the interplay between intraband and pair-exchange couplings.

DOI: 10.1103/PhysRevB.102.220504

The discovery of unconventional superconductors, which started with heavy fermions, followed by organic superconductors, and then by cuprate compounds, has prompted an era of tremendous growth of activities in condensed matter research [1,2]. The complex structure of the order parameter in these systems brought a plethora of unique phenomena and effects, with no counterparts in conventional superconductors, such as a broken time-reversal symmetry, collective modes, and an unusual Josephson effect [3–5]. The new degrees of freedom in multicomponent and multiband superconductors have been anticipated to be a promising root toward the realization of room-temperature superconductivity [6]. Such unconventional superconductors can exhibit anomalous normal-state characteristics above their critical temperature T_c, which are interpreted as the pseudogap state [7,8], corresponding to the presence of gaplike features above T_c but with a finite spectral intensity at low frequencies [9]. The origin of the pseudogap is a key for understanding the pairing glue in unconventional superconductors. Pseudogap effects have also been discussed in the context of the Bardeen-Cooper-Schrieffer (BCS) to Bose-Einstein condensation (BEC) crossover, where the BCS state of overlapping Cooper pairs changes continuously to the BEC of tightly bound molecules with increasing attractive interaction [13–22]. It is experimentally achieved in ultracold Fermi atomic gases exploiting Fano-Feshbach resonances [23–25]. Also, ultracold Fermi gases in the BCS-BEC crossover regime exhibit strong pairing fluctuations and pseudogap effects [26–29].

Among unconventional superconductors, the recently discovered iron-based superconducting compounds attract attention, since some of them are expected to be placed in the BCS-BEC crossover regime due to their large ratio between the superconducting gap and the Fermi energy [30–33]. This new class of superconductors opens a new frontier for the study of the multiband BCS-BEC crossover, where nontrivial features have been discussed [34–47]. As for other unconventional superconductors, there is now expanding experimental evidence that a pseudogap is realized in iron-based compounds [48–52], despite some reports about the absence of strong pairing fluctuations and pseudogap effects [53,54]. In order to understand the controversial pseudogap physics in multiband and multicomponent systems such as iron-based superconductors, a unified description of the multiband BCS-BEC crossover is required. Such a theory can be useful to describe also many-body physics in Yb Fermi gases near the orbital Feshbach resonance [55–63], thus bridging these atomic systems with multiband superconductors. The multichannel many-body theory is also of importance to unveil pairing properties in nanostructured superconductors [34,35,64] and electron-hole systems [65–67].

In this Rapid Communication, we develop a theory of the two-band BCS-BEC crossover in the normal state above T_c based on the T-matrix approach [68], which has been successfully applied to strongly interacting attractive Fermi gases [69]. We address the single-particle density of states (DOS) and elucidate competing mechanisms of screening and enhancement of the pseudogap in two-band systems. The

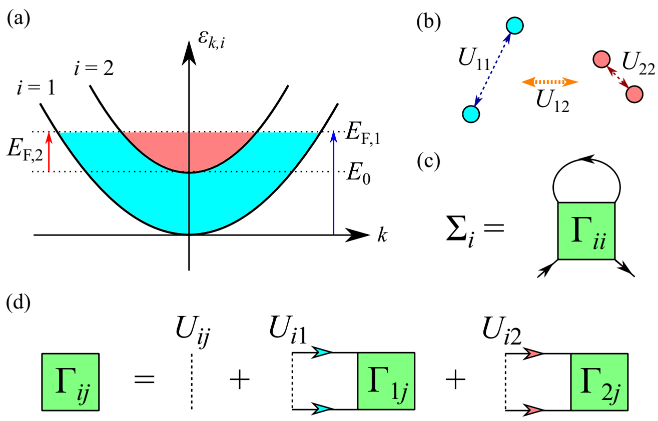

FIG. 1. (a) Two-band electronic structure considered in this work. The two bands ($i = 1, 2$) are separated in energy by E_0. Resulting Fermi energies $E_{F,i}$ have the relation $E_{F,1} = E_{F,2} + E_0$. (b) Illustration of how the interactions U_{ij} work in our configuration. While U_{11} and U_{22} cause intraband Cooper pairing in each band, U_{12} ($= U_{21}$) introduces pair tunneling between the two bands. (c) and (d) show Feynman diagrams for the self-energy Σ_i and the multiband T-matrix Γ_{ij} in our T-matrix approach, respectively.

screening of pairing fluctuations and the resulting reduction of the pseudogap regime are found in our results at the unitarity limit of the shallow band for weak pair-exchange couplings. This result suggests that, in the two-band system, the Fulde-Ferrel-Larkin-Ovchinnikov state [70,71], tending to be disrupted by pairing fluctuations [72,73], is more stable compared to the single-band case, as observed in recent experiments [74,75].

On the other hand, strong pair-exchange coupling leads to multiple pseudogaps and the emergence of binary preformed Cooper pairs in the crossover regime. This is in contrast with the pseudogap in ultracold Fermi gases, which is induced by strong intraband couplings. Hereafter, we take $\hbar = k_B = 1$ and the unit volume. As shown in Fig. 1(a), we consider a two-band model where the second shallow band ($i = 2$) is coupled with the first deep band ($i = 1$) [76,77], as described by the Hamiltonian [78]

$$H = \sum_{\boldsymbol{k},\sigma,i} \xi_{\boldsymbol{k},i} c^\dagger_{\boldsymbol{k},\sigma,i} c_{\boldsymbol{k},\sigma,i} + \sum_{i,j} U_{ij} \sum_{\boldsymbol{q}} B^\dagger_{\boldsymbol{q},i} B_{\boldsymbol{q},j}, \qquad (1)$$

where $\xi_{\boldsymbol{k},i} = k^2/(2m_i) - \mu + E_0\delta_{i,2}$ is the kinetic energy measured from the chemical potential μ with the energy separation E_0 between two bands and $\delta_{i,2}$ is the Kronecker delta. We use equal effective masses $m = m_1 = m_2$, for simplicity. $c_{\boldsymbol{k},\sigma,i}$ and $B_{\boldsymbol{q},i} = \sum_{\boldsymbol{k}} c_{-\boldsymbol{k}+\boldsymbol{q}/2,\downarrow,i} c_{\boldsymbol{k}+\boldsymbol{q}/2,\uparrow,i}$ are spin-$\sigma =\uparrow,\downarrow$ fermion and spin-singlet pair annihilation operators in the i band, respectively. In this work, we use $E_0 = 0.6E_{F,1}$ where $E_{F,i} = (3\pi^2 n_i)^{\frac{2}{3}}/(2m)$ is the noninteracting Fermi energy in the i band, defined in terms of the number density n_i. The intraband couplings U_{ii} can be characterized in terms of the intraband scattering lengths a_{ii} as

$$\frac{m}{4\pi a_{ii}} = \frac{1}{U_{ii}} + \sum_{\boldsymbol{k}}^{k_0} \frac{m}{k^2}, \qquad (2)$$

where k_0 is the momentum cutoff taken to be $100k_{F,t}$. Here, $k_{F,t} \equiv \sqrt{2mE_{F,t}}$ is the Fermi wave vector associated with the total Fermi energy $E_{F,t} = (3\pi^2 n)^{2/3}/(2m)$, defined in terms of the total number density n. In a similar way, one defines the Fermi wave vectors $k_{F,i}$ in each band, which are used to define the dimensionless intraband coupling strengths $(k_{F,1}a_{11})^{-1}$ and $(k_{F,2}a_{22})^{-1}$. In this work, we use $(k_{F,1}a_{11})^{-1} \leqslant -2$ and $-1 \leqslant (k_{F,2}a_{22})^{-1} \leqslant 1$. With this choice of couplings, pairs forming in the deep band ($i = 1$) have a BCS character, while the BCS-BEC crossover is tuned in the shallow band ($i = 2$). Although we consider a three-dimensional (3D) system, it is expected to be relevant to FeSe multiband superconductors since recent experiments exhibit a 3D wave-vector dependence of the superconducting gap [79], indicating that a 3D theoretical approach is applicable. In addition, the strong-coupling regime from the unitarity to the BEC side in 3D would be similar to the 2D counterpart due to the presence of a two-body bound state. For convenience, we also introduce a dimensionless pair-exchange coupling $\lambda_{12} = U_{12}(k_0/k_{F,t})^2 n/E_{F,t}$ where $U_{21} = U_{12}$ [76,77].

The i-band self-energy in the multiband T-matrix approach reads

$$\Sigma_i(\boldsymbol{k}, i\omega_s) = T \sum_{\boldsymbol{q},i\nu_l} \Gamma_{ii}(\boldsymbol{q}, i\nu_l) G^0_i(\boldsymbol{q} - \boldsymbol{k}, i\nu_l - i\omega_s), \qquad (3)$$

where $\omega_s = (2s + 1)\pi T$ and $\nu_l = 2l\pi T$ (s and l integers) are fermionic and bosonic Matsubara frequencies, respectively. $G^0_i(\boldsymbol{k}, i\omega_s) = [i\omega_s - \xi_{\boldsymbol{k},i}]^{-1}$ is the bare Green's function. The many-body T-matrix $\{\Gamma_{ij}\}_{2\times 2}$, which sums up the ladder-type diagram shown in Fig. 1(d), is given by

$$\Gamma_{ij}(\boldsymbol{q}, i\nu_l) = U_{ij} + \sum_{\ell=1,2} U_{i\ell}\Pi_{\ell\ell}(\boldsymbol{q}, i\nu_l)\Gamma_{\ell j}(\boldsymbol{q}, i\nu_l), \qquad (4)$$

where $\Pi_{\ell\ell}$ is

$$\Pi_{\ell\ell}(\boldsymbol{q}, i\nu_l) = -T \sum_{\boldsymbol{p},i\omega_s} G^0_i(\boldsymbol{p} + \boldsymbol{q}, i\omega_s + i\nu_l) G^0_i(\boldsymbol{p}, -i\omega_s). \qquad (5)$$

Fixing μ by solving the number equation $n = n_1 + n_2$ with

$$n_i = 2T \sum_{\boldsymbol{k},i\omega_s} G_i(\boldsymbol{k}, i\omega_s), \qquad (6)$$

where $G_i(\boldsymbol{k}, i\omega_s) = [i\omega_s - \xi_{\boldsymbol{k},i} - \Sigma_i(\boldsymbol{k}, i\omega_s)]^{-1}$ is the dressed Green's function, we obtain the superfluid/superconducting critical temperature T_c from the Thouless criterion [80] $[\Gamma_{22}(\boldsymbol{q} = 0, i\nu_l = 0)]^{-1} = 0$. [While in the presence of U_{12}, all the matrix elements $\Gamma_{ij}(\boldsymbol{q} = 0, i\nu_l = 0)$ diverge simultaneously at T_c, in the case of vanishing U_{12} only Γ_{22} diverges, due to our choice of coupling strengths.]We numerically evaluated the Matsubara frequency sum in Eqs. (3) and (6) with finite cutoffs [81] and checked their convergences [82].

The DOS is obtained from

$$N_i(\omega) = -\frac{1}{\pi} \sum_{\boldsymbol{k}} \mathrm{Im}\, G_i(\boldsymbol{k}, i\omega_s \to \omega + i\delta), \qquad (7)$$

where we take $\delta = O(10^{-3})E_{F,t}$. For simplicity, the analytic continuation is numerically performed by using the method of Padè approximants [82,83] (see Supplemental Material [82]).

Figure 2 shows the DOS $N_i(\omega)$ in the multiband BCS-BEC crossover. In the case of $\lambda_{12} = 0$, while the small intraband coupling in the deep band $(k_{F,1}a_{11})^{-1} = -4$ does

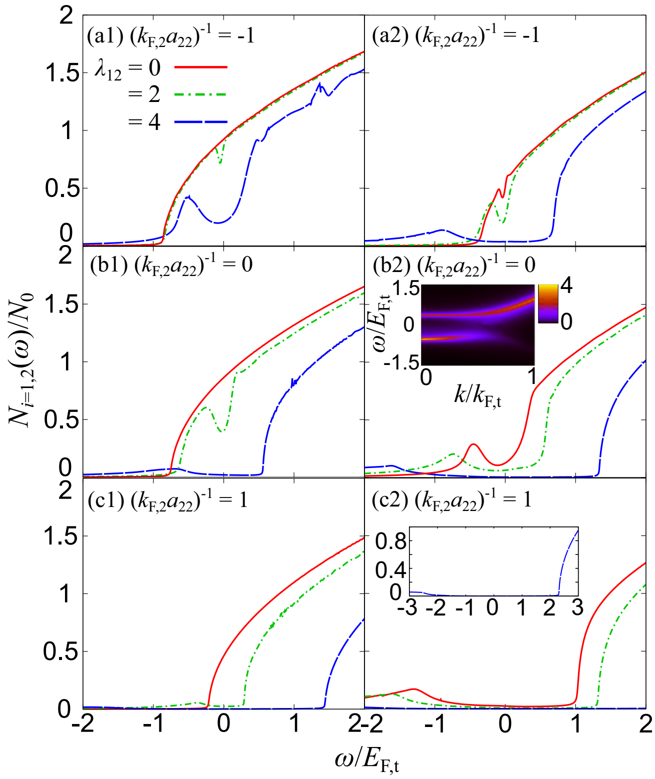

FIG. 2. DOS $N_{i=1,2}(\omega)$ at $T = T_c$ in the multiband BCS-BEC crossover. The left (right) panels show $N_1(\omega)$ [$N_2(\omega)$] at weak coupling $(k_{\rm F,2}a_{22})^{-1} = -1$ [(a1), (a2)], unitarity $(k_{\rm F,2}a_{22})^{-1} = 0$ [(b1), (b2)], and strong coupling $(k_{\rm F,2}a_{22})^{-1} = 1$ [(c1), (c2)]. In all panels, we fix $(k_{\rm F,1}a_{11})^{-1} = -4$. The dimensionless pair-exchange coupling is taken as $\lambda_{12} = 0$, 2, and 4. For reference, we present the spectral weight $A_2(\boldsymbol{k}, \omega)E_{\rm F,t} = -{\rm Im}\, G_2(\boldsymbol{k}, \omega + i\delta)E_{\rm F,t}/\pi$ at $\lambda_{12} = 0.5$ in the inset of (b2). The inset of (c2) shows $N_2(\omega)$ at $\lambda_{12} = 4$ because of the large energy gap. $N_0 = mk_{\rm F,t}^2/(2\pi^2)$ is the noninteracting DOS associated with total number density n.

not suppress a square-root behavior typical of noninteracting gases, $N_0(\omega) \propto \sqrt{\omega + \mu}$, $N_2(\omega)$ exhibits the pseudogap around $\omega = 0$ [84] due to strong pairing fluctuations associated with U_{22}. It is consistent with the results obtained in the single-band counterpart. On the other hand, in the presence of nonzero pair-exchange coupling, $N_1(\omega)$ also shows a pseudogapped DOS even with weak intraband coupling. This is thus a “pair-exchange-induced pseudogap.” In addition, the coupling λ_{12} enlarges the pseudogap in $N_2(\omega)$. The pair-exchange-induced pseudogap in $N_1(\omega)$ becomes larger when the intraband coupling in the shallow band $(k_{\rm F,2}a_{22})^{-1}$ gets stronger. Eventually, at very strong pair-exchange coupling such as $\lambda_{12} = 4$, both $N_1(\omega)$ and $N_2(\omega)$ show a fully gapped structure due to the large two-body binding energy.

These features can be qualitatively understood as follows. Quite generally, the size of pseudogap effects in the band i can be roughly estimated by the energy scale $\Delta_{\infty,i}^2 = -T\sum_{\boldsymbol{q},i\nu_l}\Gamma_{ii}(\boldsymbol{q}, i\nu_l)$ introduced in Ref. [85] for a single band, and here generalized to the multiband case. Even though in general Δ_∞ is related to the so-called Tan’s contact C [86], it was shown in Ref. [87] that in the intermediate crossover regime and close to T_c, Δ_∞ is close to the pseudogap scale

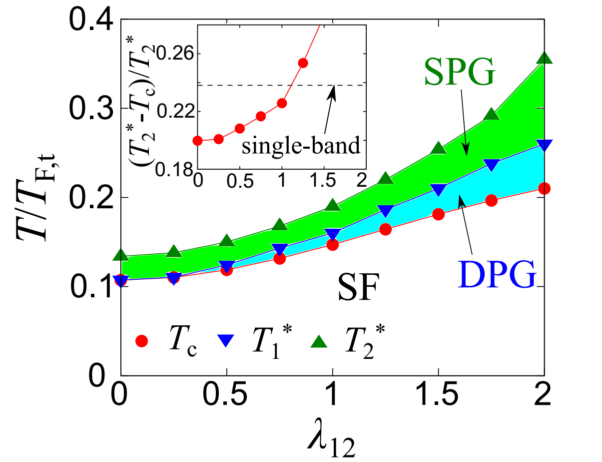

FIG. 3. The band-dependent pseudogap temperatures $T_{i=1,2}^*$ and the critical temperature T_c as functions of λ_{12}. The intraband couplings are chosen as $(k_{\rm F,2}a_{22})^{-1} = 0$ and $(k_{\rm F,1}a_{11})^{-1} = -2$. The regions where $T_c < T < T_1^*$ and $T_1^* < T < T_2^*$ are double-pseudogap (DPG) and single-pseudogap (SPG) regimes, respectively. The inset shows the ratio $(T_2^* - T_c)/T_c$ as a function of λ_{12} which characterizes how the pseudogap regime in the shallow band is shrunk by multiband effects. The horizontal dashed line in the inset shows the single-band counterpart.

energy determined from $N(\omega)$. In the two-band case in the presence of a finite λ_{12}, $\Gamma_{11}(\boldsymbol{q}, i\nu_l)$ and $\Gamma_{22}(\boldsymbol{q}, i\nu_l)$ diverge simultaneously at T_c, for $\boldsymbol{q} = 0$ and $\nu_l = 0$. For this reason, the scales $\Delta_{\infty,1}$ and $\Delta_{\infty,2}$ become interconnected, explaining in this way the pair-exchange-induced pseudogap in the deep band.

To characterize the pseudogap state, we introduce the band-dependent pseudogap temperatures $T_{i=1,2}^*$ where the minimum of $N_i(\omega)$ around $\omega = 0$ disappears [26]. Figure 3 shows the obtained phase diagram at unitarity (crossover regime) of the shallow band coupled with the weakly interacting deep band, where $(k_{\rm F,2}a_{22})^{-1} = 0$ and $(k_{\rm F,1}a_{11})^{-1} = -2$. In this figure, we plot the critical temperature T_c and pseudogap temperatures $T_{1,2}^*$ as functions of λ_{12}. While the single pseudogap (SPG) appears in the region $T_1^* < T < T_2^*$, the double pseudogaps (DPGs) can be found below $T = T_1^*$. In the case of vanishing λ_{12}, since the deep band does not exhibit pseudogap behavior, we obtain $T_1^* = T_c$. However, if λ_{12} is shifted from zero to strong coupling, T_1^* deviates from T_c due to the interband pairing fluctuations. Thus, the pseudogap regime in the deep band ($T_c < T < T_2^*$) originates purely from the pseudogap induced by the transfer of pair fluctuations due to the pair exchange (rise of an induced pseudogap).

The inset of Fig. 3 shows the ratio $(T_2^* - T_c)/T_c$ as a function of λ_{12}. For a reference, we plot in this figure the numerical value obtained in the single-band counterpart at the unitarity limit. The pseudogap regime ($T_c < T < T_2^*$) in the two-band case with small λ_{12} is clearly reduced compared to the single-band counterpart (fall of the pseudogap). This tendency is consistent with the experiments for FeSe multiband superconductors in the BCS-BEC crossover regime [53,54] as well as with previous theoretical work [44,76]. This screening effect is related to the Pauli blocking produced by the large

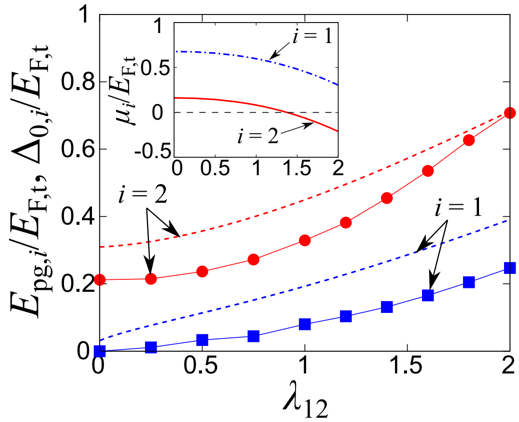

FIG. 4. The pseudogap sizes $E_{\mathrm{pg},i}$ estimated from the single-particle DOS at $T=T_{\mathrm{c}}$ (symbols) are compared with the mean-field gaps $\Delta_{0,i}$ at $T=0$ (dashed lines) as a function of the dimensionless pair-exchange coupling λ_{12}. The intraband interaction parameters are chosen as $(k_{\mathrm{F},2}a_{22})^{-1}=0$ and $(k_{\mathrm{F},1}a_{11})^{-1}=-2$. The inset shows the chemical potential $\mu_i \equiv \mu - E_0\delta_{i,2}$ referred to the bottom of each band.

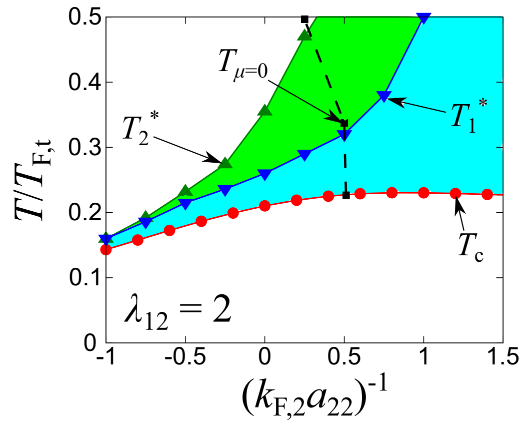

FIG. 5. Two-band BCS-BEC crossover phase diagram in the temperature vs intraband coupling $(k_{\mathrm{F},2}a_{22})^{-1}$ plane for a strong pair-exchange coupling $\lambda_{12}=2$ and $(k_{\mathrm{F},1}a_{11})^{-1}=-2$. $T_{\mu=0}$ shows the temperature where $\mu=0$.

Fermi surface in the deep band for our two-band configuration [39]. However, such a regime is destroyed if one shifts λ_{12} to the strong-coupling regime ($\lambda_{12} \gtrsim 1$) due to strong interband pairing fluctuations.

Figure 4 shows a comparison between the pseudogap energies $E_{\mathrm{pg},i}$ obtained from our T-matrix approach at $T=T_{\mathrm{c}}$ and the mean-field gaps $\Delta_{0,i}$ at $T=0$ [77]. Here, $E_{\mathrm{pg,i}}$ is the half width of the dip structure in $N_i(\omega)$ around $\omega=0$. Specifically, we define $E_{\mathrm{pg},i}=(\omega_i'-\omega_{\mathrm{LM},i})/2$, where $\omega_{\mathrm{LM},i}<0$ is the frequency where $N_i(\omega)$ has a local maximum due to the pseudogap and $\omega_i'>0$ is determined such that $N_i(\omega_i')=N_i(\omega_{\mathrm{LM},i})$ [26,88]. The dependences of $E_{\mathrm{pg},i}$ and $\Delta_{0,i}$ on λ_{12} are qualitatively similar. As for the single-band BCS-BEC crossover, the pseudogap can be regarded as half the energy needed to excite a single-particle by breaking a preformed Cooper pair. The coexistence and different magnitudes of the pseudogap energies $E_{\mathrm{pg},1}$ and $E_{\mathrm{pg},2}$ indicate the emergence of binary preformed Cooper pairs. It is consistent with our prediction of binary molecular BEC with different pair sizes in the strong-coupling regime [76]. Indeed, different intraband pair-correlation lengths, corresponding to different Cooper-pair sizes in each band, are obtained also within the mean-field approach at $T=0$ [77]. In addition, this picture is supported by the emergence of binary Tan's contacts characterizing two kinds of pair correlations in the two-band system [68]. The finding that $E_{\mathrm{pg},i}$ is smaller compared to $\Delta_{0,i}$ is also consistent with the single-band result [88]. We note that in the strong pair-exchange coupling regime $\lambda_{12} \gtrsim 1.5$, $\mu_2=\mu-E_0$ changes its sign (where $\mu_i=\mu-E_0\delta_{i,2}$ is the chemical potential measured from the bottom of each band) due to the large two-body binding energy associated with U_{22} as well as with λ_{12} (see the inset of Fig. 4). In such a regime, $N_i(\omega)$ exhibits a fully gapped structure and $E_{\mathrm{pg},i}$ progressively approaches the two-body binding energy. Although not shown here, μ_1 also changes sign in the stronger coupling regime. Finally, we report the phase diagram of the two-band BCS-BEC crossover for strong pair-exchange coupling $\lambda_{12}=2$, as shown in Fig. 5. At weak intraband couplings, two pseudogaps simultaneously open in the two bands. These multiple pseudogaps originate from the strong pair-exchange coupling. On the other hand, when the intraband coupling in the shallow band increases, the two pseudogap temperatures deviate from each other, indicating multiple energy scales of pseudogaps as shown in Fig. 4. This multiple pseudogap regime evolves eventually into a molecular binary Bose gas regime. Although the boundaries between these regimes are not sharp, the temperature $T_{\mu=0}$ at which the chemical potential μ goes below the bottom of the deep band could be used as a qualitative crossover line separating the two regimes at low temperature.

In conclusion, we have demonstrated how multiple pseudogaps appear and when pair fluctuations are screened in the two-band BCS-BEC crossover at arbitrary pair-exchange couplings. While the pair fluctuations inducing the pseudogap are screened by multiband effects at weak pair-exchange couplings, this screening regime turns into multiple pseudogaps at strong pair exchanges due to interband pairing fluctuations. We have constructed the phase diagram of the two-pseudogap state in the temperature and pair-exchange plane, and show the pseudogap temperatures where single and multiple pseudogaps appear in the single-particle density of states. Examining the pseudogap temperature in the shallow band, we have confirmed that the screening of pairing fluctuations due to the multiband nature can be found in the BCS-BEC crossover regime. Furthermore, the different magnitudes of the pseudogaps indicate the presence of binary preformed Cooper pairs with different binding energies and sizes, as also confirmed from the comparison between the pseudogap size at the critical temperature and the mean-field energy gaps at $T=0$.

We believe our results to be quite general: By relaxing, if required, some restrictions of the model considered here, such as the fixed energy shift and the electronlike character of the bands, the idea of multichannel pairing fluctuations could be applied to a variety of strongly correlated multicomponent systems such as cold atoms, electron-hole systems, nuclear matter, and nanostructured materials.

H.T. is grateful for the hospitality of the Physics Division at University of Camerino. H.T. was supported by Grant-in-Aid for JSPS fellows (No.17J03975) and for Scientific Research from JSPS (No.18H05406).

[1] D. J. Scalapino, A common thread: The pairing interaction for unconventional superconductors, Rev. Mod. Phys. **84**, 1383 (2012).

[2] M. Zehetmayer, A review of two-band superconductivity: materials and effects on the thermodynamic and reversible mixed-state properties, Supercond. Sci. Technol. **26**, 043001 (2013).

[3] S.-Z. Lin, Ground state, collective mode, phase soliton and vortex in multiband superconductors, J. Phys.: Condens. Matter **26**, 493202 (2014).

[4] Y. Tanaka, Multicomponent superconductivity based on multiband superconductors, Supercond. Sci. Technol. **28**, 034002 (2015).

[5] Y. Yerin and A. N. Omelyanchouk, Proximity and Josephson effects in microstructures based on multiband superconductors, Low Temp. Phys. **43**, 1013 (2017).

[6] M. V. Milošević and A. Perali, Emergent phenomena in multicomponent superconductivity: An introduction to the focus issue, Supercond. Sci. Technol. **28**, 060201 (2015).

[7] Ø. Fischer, M. Kugler, I. Maggio-Aprile, C. Berthod, and C. Renner, Scanning tunneling spectroscopy of high-temperature superconductors, Rev. Mod. Phys. **79**, 353 (2007).

[8] E. J. Mueller, Review of pseudogaps in strongly interacting Fermi gases, Rep. Prog. Phys. **80**, 104401 (2017).

[9] We exclude here from our consideration some exceptions like strongly disordered conventional *s*-wave superconductors such as TiN [10], NbN [11], and granular aluminum [12].

[10] B. Sacépé, C. Chapelier, T. I. Baturina, V. M. Vinokur, M. R. Baklanov, and M. Sanquer, Pseudogap in a thin film of a conventional superconductor, Nat. Commun. **1**, 140 (2010).

[11] M. Mondal, A. Kamlapure, M. Chand, G. Saraswat, S. Kumar, J. Jesudasan, L. Benfatto, V. Tripathi, and P. Raychaudhuri, Phase Fluctuations in a Strongly Disordered *s*-Wave NbN Superconductor Close to the Metal-Insulator Transition, Phys. Rev. Lett. **106**, 047001 (2011).

[12] U. S. Pracht, N. Bachar, L. Benfatto, G. Deutscher, E. Farber, M. Dressel, and M. Scheffler, Shaping a superconducting dome: Enhanced Cooper pairing versus suppressed phase coherence in coupled aluminum nanograins, Phys. Rev. B **93**, 100503(R) (2016).

[13] D. M. Eagles, Possible pairing without superconductivity at low carrier concentrations in bulk and thin-film superconducting semiconductors, Phys. Rev. **186**, 456 (1969).

[14] A. J. Leggett, Diatomic molecules and Cooper pairs, in *Modern Trends in the Theory of Condensed Matter*, edited by A. Peralski and R. Przystawa (Springer, Berlin, 1980).

[15] P. Nozières and S. Schmitt-Rink, Bose condensation in an attractive fermion gas: From weak to strong coupling superconductivity, J. Low Temp. Phys. **59**, 195 (1985).

[16] C. A. R. Sá de Melo, M. Randeria, and J. R. Engelbrecht, Crossover from BCS to Bose Superconductivity: Transition Temperature and Time-Dependent Ginzburg-Landau Theory, Phys. Rev. Lett. **71**, 3202 (1993).

[17] A. Perali, P. Pieri, G. C. Strinati, and C. Castellani, Pseudogap and spectral function from superconducting fluctuations to the bosonic limit, Phys. Rev. B **66**, 024510 (2002).

[18] Y. Ohashi and A. Griffin, BCS-BEC Crossover in a Gas of Fermi Atoms with a Feshbach Resonance, Phys. Rev. Lett. **89**, 130402 (2002).

[19] S. Giorgini, L. P. Pitaevskii, and S. Stringari, Theory of ultracold atomic Fermi gases, Rev. Mod. Phys. **80**, 1215 (2008).

[20] I. Bloch, J. Dalibard, and W. Zwerger, Many-body physics with ultracold gases, Rev. Mod. Phys. **80**, 885 (2008).

[21] G. C. Strinati, P. Pieri, G. Röpke, P. Schuck, and M. Urban, The BCS-BEC crossover: From ultra-cold Fermi gases to nuclear systems, Phys. Rep. **738**, 1 (2018).

[22] Y. Ohashi, H. Tajima, and P. van Wyk, BCS-BEC crossover in cold atomic and in nuclear systems, Prog. Nucl. Part. Phys. **111**, 103739 (2020).

[23] C. A. Regal, M. Greiner, and D. S. Jin, Observation of Resonance Condensation of Fermionic Atom Pairs, Phys. Rev. Lett. **92**, 040403 (2004).

[24] M. Bartenstein, A. Altmeyer, S. Riedl, S. Jochim, C. Chin, J. H. Denschlag, and R. Grimm, Crossover from a Molecular Bose-Einstein Condensate to a Degenerate Fermi Gas, Phys. Rev. Lett. **92**, 120401 (2004).

[25] M. W. Zwierlein, C. A. Stan, C. H. Schunck, S. M. F. Raupach, A. J. Kerman, and W. Ketterle, Condensation of Pairs of Fermionic Atoms near a Feshbach Resonance, Phys. Rev. Lett. **92**, 120403 (2004).

[26] S. Tsuchiya, R. Watanabe, and Y. Ohashi, Single-particle properties and pseudogap effects in the BCS-BEC crossover regime of an ultracold Fermi gas above T_c, Phys. Rev. A **80**, 033613 (2009).

[27] J. P. Gaebler, J. T. Stewart, T. E. Drake, D. S. Jin, A. Perali, P. Pieri, and G. C. Strinati, Observation of pseudogap behaviour in a strongly interacting Fermi gas, Nat. Phys. **6**, 569 (2010).

[28] A. Perali, F. Palestini, P. Pieri, G. C. Strinati, J. T. Stewart, J. P. Gaebler, T. E. Drake, and D. S. Jin, Evolution of the Normal State of a Strongly Interacting Fermi Gas from a Pseudogap Phase to a Molecular Bose Gas, Phys. Rev. Lett. **106**, 060402 (2011).

[29] F. Palestini, A. Perali, P. Pieri, and G. C. Strinati, Dispersions, weights, and widths of the single-particle spectral function in the normal phase of a Fermi gas, Phys. Rev. B **85**, 024517 (2012).

[30] K. Okazaki, Y. Ito, Y. Ota, Y. Kotani, T. Shimojima, T. Kiss, S. Watanabe, C.-T. Chen, S. Niitaka, T. Hanaguri, H. Takagi, A. Chainani, and S. Shin, Superconductivity in an electron band just above the Fermi level: possible route to BCS-BEC superconductivity, Sci. Rep. **4**, 4109 (2014).

[31] S. Kasahara, T. Watashige, T. Hanaguri, Y. Kohsaka, T. Yamashita, Y. Shimoyama, Y. Mizukami, R. Endo, and H. Ikeda, Field-induced superconducting phase of FeSe in the BCS-BEC cross-over, Proc. Natl. Acad. Sci. U.S.A. **111**, 16309 (2014).

[32] S. Kasahara, T. Yamashita, A. Shi, R. Kobayashi, Y. Shimoyama, T. Watashige, K. Ishida, T. Terashima, T. Wolf, F. Hardy, C. Meingast, H. v. Löhneysen, A. Levchenko, T. Shibauchi, and Y. Matsuda, Giant superconducting fluctuations in the compensated semimetal FeSe at the BCS-BEC crossover, Nat. Commun. **7**, 12843 (2016).
[33] S. Rinott, K. B. Chashka, A. Ribak, E. D. L. Rienks, A. Taleb-Ibrahimi, P. Le Fevre, F. Bertran, M. Randeria and A. Kanigel, Tuning across the BCS-BEC crossover in the multiband superconductor $Fe_{1+y}Se_xTe_{1-x}$: An angle-resolved photoemission study, Sci. Adv. **3**, 1602372 (2017).
[34] A. Perali, A. Bianconi, A. Lanzara, and N. L. Saini, The gap amplification at a shape resonance in a superlattice of quantum stripes: A mechanism for high T_c, Solid State Commun. **100**, 181 (1996).
[35] A. Bianconi, A. Valletta, A. Perali, and N. L. Saini, Superconductivity of a striped phase at the atomic limit, Physica C **296**, 269 (1998).
[36] M. Iskin and C. A. R. Sá de Melo, BCS-BEC crossover of a collective excitations in two-band superfluids, Phys. Rev. B **72**, 024512 (2005).
[37] M. Iskin and C. A. R. Sá de Melo, Two-band superfluidity from the BCS to the BEC limit, Phys. Rev. B **74**, 144517 (2006).
[38] L. He and P. Zhuang, Stable Sarma state in two-band Fermi systems, Phys. Rev. B **79**, 024511 (2009).
[39] A. Guidini and A. Perali, Band-edge BCS-BEC crossover in a two-band superconductor: Physical properties and detection parameters, Supercond. Sci. Technol. **27**, 124002 (2014).
[40] M. Takahashi, T. Mizushima, and K. Machida, Multiband effects on Fulde-Ferrell-Larkin-Ovchinnikov states of Pauli-limited superconductors, Phys. Rev. B **89**, 064505 (2014).
[41] L. He, H. Hu, and X.-J. Liu, Two-band description of resonant superfluidity in atomic Fermi gases, Phys. Rev. A **91**, 023622 (2015).
[42] A. V. Chubukov, I. Eremin, and D. V. Efremov, Superconductivity versus bound-state formation in a two-band superconductor with small Fermi energy: Applications to Fe pnictides/chalcogenides and doped $SrTiO_3$, Phys. Rev. B **93**, 174516 (2016).
[43] S. Wolf, A. Vagov, A. A. Shanenko, V. M. Axt, A. Perali, and J. A. Aguiar, BCS-BEC crossover induced by a shallow band: Pushing standard superconductivity types apart, Phys. Rev. B **95**, 094521 (2017).
[44] L. Salasnich, A. A. Shanenko, A. Vagov, J. A. Aguiar, and A. Perali, Screening of pair fluctuations in superconductors with coupled shallow and deep bands: A route to higher-temperature superconductivity, Phys. Rev. B **100**, 064510 (2019).
[45] S. N. Klimin, J. Tempere, G. Lombardi, and J. T. Devreese, Finite temperature effective field theory and two-band superfluidity in Fermi gases, Eur. Phys. J. B **88**, 122 (2015).
[46] S. N. Klimin, H. Kurkjian, and J. Tempere, Leggett collective excitations in a two-band Fermi superfluid at finite temperature, New J. Phys. **21**, 113043 (2019).
[47] A. A. Vargas-Paredes, A. A. Shanenko, A. Vagov, M. V. Milošević, and A. Perali, Crossband versus intraband pairing in superconductors: Signatures and consequences of the interplay, Phys. Rev. B **101**, 094516 (2020).
[48] Y. S. Kwon, J. B. Hong, Y. R. Jang, H. J Oh, Y. Y. Song, B. H. Min, T. Iizuka, S.-i. Kimura, A. V. Balatsky, and Y. Bang, Evidence of a pseudogap for superconducting iron-pnictide $Ba_{0.6+\delta}K_{0.4-\delta}Fe_2As_2$ single crystals from optical conductivity measurements, New J. Phys. **14**, 063009 (2012).
[49] M. Matusiak and T. Wolf, Violation of the Wiedemann-Franz law as an evidence of the pseudogap in the iron-based superconductor $Ba(Fe_{1-x}Co_x)_2As_2$, Phys. Rev. B **92**, 020507(R) (2015).
[50] Y. I. Seo, W. J. Choi, S. Kimura, and Y. S. Kwon, Evidence for a preformed Cooper pair model in the pseudogap spectra of a $Ca_{10}(Pt_4As_8)(Fe_2As_2)_5$ single crystal with a nodal superconducting gap, Sci. Rep. **9**, 3987 (2019)
[51] B. L. Kang, M. Z. Shi, S. J. Li, H. H. Wang, Q. Zhang, D. Zhao, J. Li, D. W. Song, L. X. Zheng, L. P. Nie, T. Wu, and X. H. Chen, Preformed Cooper Pairs in Layered FeSe-Based Superconductors, Phys. Rev. Lett. **125**, 097003 (2020).
[52] A. L. Solovjov, E. V. Petrenko, L. V. Omelchenko, E. Nazarova, K. Buchkov, and K. Rogacki, Fluctuating Cooper pairs in FeSe at temperatures exceeding double T_c, Sci. Technol. **34**, 015013 (2021).
[53] T. Hanaguri, S. Kasahara, J. Böker, I. Eremin, T. Shibauchi, and Y. Matsuda, Quantum Vortex Core and Missing Pseudogap in the Multiband BCS-BEC Crossover Superconductor FeSe, Phys. Rev. Lett. **122**, 077001 (2019).
[54] H. Takahashi, F. Nabeshima, R. Ogawa, E. Ohmichi, H. Ohta, and A. Maeda, Superconducting fluctuations in FeSe investigated by precise torque magnetometry, Phys. Rev. B **99**, 060503(R) (2019).
[55] R. Zhang, Y. Cheng, H. Zhai, and P. Zhang, Orbital Feshbach Resonance in Alkali-Earth Atoms, Phys. Rev. Lett. **115**, 135301 (2015).
[56] G. Pagano, M. Mancini, G. Cappellini, L. Livi, C. Sias, J. Catani, M. Inguscio, and L. Fallani, Strongly Interacting Gas of Two-Electron Fermions at an Orbital Feshbach Resonance, Phys. Rev. Lett. **115**, 265301 (2015).
[57] M. Höfer, L. Riegger, F. Scazza, C. Hofrichter, D. R. Fernandes, M. M. Parish, J. Levinsen, I. Bloch, and S. Fölling, Observation of an Orbital Interaction-Induced Feshbach Resonance in ^{173}Yb, Phys. Rev. Lett. **115**, 265302 (2015).
[58] M. Iskin, Two-band superfluidity and intrinsic Josephson effect in alkaline-earth-metal Fermi gases across an orbital Feshbach resonance, Phys. Rev. A **94**, 011604(R) (2016).
[59] L. He, J. Wang, S.-G. Peng, X.-J. Liu, and H. Hu, Strongly correlated Fermi superfluid near an orbital Feshbach resonance: Stability, equation of state, and Leggett mode, Phys. Rev. A **94**, 043624 (2016).
[60] J. Xu, R. Zhang, Y. Cheng, P. Zhang, R. Qi, and H. Zhai, Reaching a Fermi-superfluid state near an orbital Feshbach resonance, Phys. Rev. A **94**, 033609 (2016).
[61] M. Iskin, Trapped ^{173}Yb Fermi gas across an orbital Feshbach resonance, Phys. Rev. A **95**, 013618 (2017).
[62] P. Zou, L. He, X.-J. Liu, and H. Hu, Strongly interacting Sarma superfluid near orbital Feshbach resonance, Phys. Rev. A **97**, 043616 (2018).
[63] S. Mondal, D. Inotani, and Y. Ohashi, Single-particle excitations and strong coupling effects in the BCS-BEC crossover regime of a rare-earth Fermi gas with an orbital Feshbach resonance, J. Phys. Soc. Jpn. **87**, 084302 (2018).
[64] Y. Chen, A. A. Shanenko, A. Perali, and F. M. Peeters, Superconducting nanofilms: Molecule-like pairing induced by quantum confinement, J. Phys.: Condens. Matter **24**, 185701 (2012).

[65] Y. Tomio, K. Honda, and T. Ogawa, Excitonic BCS-BEC crossover at finite temperature: Effects of repulsion and electron-hole mass difference, Phys. Rev. B **73**, 235108 (2006).

[66] P. Pieri, D. Neilson, and G. C. Strinati, Effects of density imbalance on the BCS-BEC crossover in semiconductor electron-hole bilayers, Phys. Rev. B **75**, 113301 (2007).

[67] A. Perali, D. Neilson, and A. R. Hamilton, High-Temperature Superfluidity in Double-Bilayer Graphene, Phys. Rev. Lett. **110**, 146803 (2013).

[68] H. Tajima, A. Perali, and P. Pieri, BCS-BEC crossover and pairing fluctuations in a two band superfluid/superconductor: A T matrix approach, Condens. Matter **5**, 10 (2020).

[69] M. Pini, P. Pieri, and G. C. Strinati, Fermi gas thoughout the BCS-BEC crossover: Comparative study of t-matrix approaches with various degrees of self-consistency, Phys. Rev. B **99**, 094502 (2019).

[70] P. Fulde and R. A. Ferrell, Superconductivity in a Strong Spin-Exchange Field, Phys. Rev. **135**, A550 (1964).

[71] A. I. Larkin and Yu. N. Ovchinnikov, Nonuniform state of superconductors, Zh. Eksp. Teor. Fiz. **47**, 1136 (1964) [Sov. Phys. JETP **20**, 762 (1965)].

[72] H. Shimahara, Phase fluctuations and Kosterlitz-Thouless transition in two-fimensional Fulde-Ferrell-Larkin-Ovchinnikov superconductors, J. Phys. Soc. Jpn. **67**, 1872 (1998).

[73] Y. Ohashi, On the Fulde-Ferrell state in spatially isotropic superconductors, J. Phys. Soc. Jpn. **71**, 2625 (2002).

[74] S. Kasahara, Y. Sato, S. Licciardello, M. Culo, S. Arsenijević, T. Ottenbros, T. Tominaga, J. Böker, I. Eremin, T. Shibauchi, J. Wosnitza, N. E. Hussey, and Y. Matsuda, Evidence for an Fulde-Ferrell-Larkin-Ovchinnikov State with Segmented Vortices in the BCS-BEC-Crossover Superconductor FeSe, Phys. Rev. Lett. **124**, 107001 (2020).

[75] S. Molatta, D. Opherden, J. Wosnitza, Z. T. Zhang, T. Wolf, H. v. Löhneysen, R. Sarkar, P. K. Biswas, H.-J. Grafe, and H. Kühne, Superconductivity of highly spin-polarized electrons in FeSe probed by ^{77}Se NMR, arXiv:2010.10128.

[76] H. Tajima, Y. Yerin, A. Perali, and P. Pieri, Enhanced critical temperature, pairing fluctuation effects, and BCS-BEC crossover in a two-band Fermi gas, Phys. Rev. B **99**, 180503(R) (2019).

[77] Y. Yerin, H. Tajima, P. Pieri, and A. Perali, Coexistence of giant Cooper pairs with a bosonic condensate and anomalous behavior of energy gaps in the BCS-BEC crossover of a two-band superfluid Fermi gas, Phys. Rev. B **100**, 104528 (2019).

[78] H. Suhl, B. T. Matthias, and L. R. Walker, Bardeen-Cooper-Schrieffer Theory of Superconductivity in the Case of Overlapping Bands, Phys. Rev. Lett. **3**, 552 (1959).

[79] Y. S. Kushnirenko, A. V. Fedorov, E. Haubold, S. Thirupathaiah, T. Wolf, S. Aswartham, I. Morozov, T. K. Kim, B. Büchner, and S. V. Borisenko, Three-dimensional superconducting gap in FeSe from angle-resolved photoemission spectroscopy, Phys. Rev. B **97**, 180501(R) (2018).

[80] D. J. Thouless, Perturbation theory in statistical mechanics and the theory of superconductivity, Ann. Phys. **10**, 553 (1960).

[81] P. Pieri, L. Pisani, and G. C. Strinati, BCS-BEC crossover at finite temperature in the broken-symmetry phase, Phys. Rev. B **70**, 094508 (2004).

[82] See Supplemental Material at http://link.aps.org/supplemental/10.1103/PhysRevB.102.220504 for the analytic continuation with the Padè approximants and the cutoff dependence.

[83] H. J. Vidberg and J. W. Serene, Solving the Eliashberg equations by means of N-point Padé approximants, J. Low Temp. Phys. **29**, 179 (1977).

[84] N. Trivedi and M. Randeria, Deviations from Fermi-Liquid Behavior above T_c in 2D Short Coherence Length Superconductors, Phys. Rev. Lett. **75**, 312 (1995).

[85] P. Pieri, A. Perali, and G. C. Strinati, Enhanced paraconductivity-like fluctuations in the radio frequency spctra of ultracold Fermi atoms, Nat. Phys. **5**, 736 (2009).

[86] S. Tan, Energetics of a strongly correlated Fermi gas, Ann. Phys. **323**, 2952 (2008); S. Tan, Large momentum part of a strongly correlated Fermi gas, Ann. Phys. **323**, 2971 (2008).

[87] F. Palestini, A. Perali, P. Pieri, and G. C. Strinati, Temperature and coupling dependence of the universal contact intensity for an ultracold Fermi gas, Phys. Rev. A **82**, 021605(R) (2010).

[88] R. Watanabe, S. Tsuchiya, and Y. Ohashi, Superfluid density of states and pseudogap phenomenon in the BCS-BEC crossover regime of a superfluid Fermi gas, Phys. Rev. A **82**, 043630 (2010).